Compact Quasi-Periodic and Aperiodic TE_{0n} Mode Converters in Overmoded Circular Waveguides for Use with Gyrotrons

MICHAEL J. BUCKLEY, MEMBER, IEEE, AND RONALD J. VERNON, MEMBER, IEEE

Abstract—**Designs of compact quasi-periodic and aperiodic TE_{0n}–TE_{0n-1} circular waveguide converters for use with gyrotrons in an electron cyclotron heating (ECH) system are developed by analytically and numerically solving the coupled-mode differential equations. Quasi-periodic mode transducer designs are developed which convert the TE_{02} mode to the TE_{01} mode and in some cases include a taper (waveguide radius reduction). A 60 GHz aperiodic mode converter–taper combines a 6.35 cm–2.779 cm waveguide diameter taper and a TE_{02}–TE_{01} mode converter. A 140 GHz aperiodic mode converter–taper combines a 6.35 cm–2.779 cm waveguide diameter taper and a TE_{03}–TE_{02}–TE_{01} mode converter. The resulting designs are highly efficient (conversion efficiencies $\geq$ 99.4%), are shorter, have a broader bandwidth than previous designs, and have a waveguide radius greater than or equal to 1.389 cm over the entire length of the transducer to allow for high-power transmission. Experimental results which are consistent with theoretical calculations are presented.**

I. Introduction

GYROTRONS are an efficient source of high-power millimeter-wavelength energy. With output powers that reach above 200 kW and frequencies that range from 28 to 140 GHz and beyond, gyrotrons have been used to heat magnetically confined plasmas at the electron cyclotron resonance frequency [1], [2]. First-generation gyrotrons typically have an output in an axially symmetric TE_{0n} mode in a 6.35-cm-diameter circular waveguide. This is usually converted into a linearly polarized mode by means of one or more mode converters. In order to make mode converters of reasonable length, the waveguide diameter is often tapered to a 2.779 cm diameter.

One typical series of mode transducers is TE_{0n}-to-TE_{01}, TE_{01}-to-TE_{11}, and then TE_{11}-to-HE_{11}. The HE_{11} mode is a completely linearly polarized mode which is an eigenmode of a corrugated waveguide. Because of the large amounts of power produced by the gyrotron, the waveguide carrying its output must have a large diameter and thus is highly overmoded. Using the technique of periodic waveguide perturbations developed by Kovalev *et al.* [3], other workers have designed mode transducers which successfully convert the output of a gyrotron into the linearly polarized HE_{11} mode. These mode converters suffer from the drawback of being relatively long and having relatively narrow bandwidths or of having radii less than 1.389 cm, which limits power handling capability [1], [2], [4]. In this paper, we discuss techniques for designing compact quasi-periodic and aperiodic TE_{0n}–TE_{0n-1} mode transducers with radii greater than or equal to 1.389 cm [5], [6]. The quasi-periodic mode transducers convert the TE_{0n} mode to the TE_{0n-1} mode and in some cases include a small taper. The aperiodic mode transducers convert the TE_{0n} mode into the TE_{0n-1} mode and include a 6.35 cm to 2.779 cm waveguide diameter taper.

Manuscript received January 18, 1989; revised January 9, 1990. This work was supported by the U.S Department of Energy under Contract DE-FG02-85ER52122 and the National Magnetic Fusion Energy Computer Center.

M. J. Buckley was with the Department of Electrical and Computer Engineering, University of Wisconsin, Madison, WI 53706. He is now with Texas Instruments, McKinney, TX 75070.

R. J. Vernon is with the Department of Electrical and Computer Engineering, University of Wisconsin, Madison, WI 53706.

IEEE Log Number 9034883.

II. TE_{0n}–TE_{0q} Coupled-Mode Equations

The TE_{0n}–TE_{0q} coupled-mode equations were derived by Unger [7] using techniques pioneered by Schelkunoff [8]. The coupled-mode equations, neglecting reflected modes, can be written in the form

$$\frac{dA_n^+}{dz} = -i\beta_n(z)A_n^+ + \sum_{\substack{q \\ q \neq n}} T_{nq}(z)A_q^+ \qquad (1)$$

where

$$T_{nq}(z) = \frac{1}{a}\frac{da}{dz}\frac{\chi'_{0n}\chi'_{0q}}{\chi'^2_{0n} - \chi'^2_{0q}}\left[(\beta_n/\beta_q)^{1/2} + (\beta_q/\beta_n)^{1/2}\right].$$

The power transported in the $+\hat{z}$ direction by the nth mode at the point z is given by $|A_n^+|^2$, a is the radius (as a function of z) of the mode converter, χ'_{0n} is the nth zero of $J'_0(x)$ (excluding the one at $x=0$), and $\beta_n = \sqrt{k^2 - (\chi'_{0n}/a)^2}$, where k is the free-space wavenumber. The beat wavenumber is defined as $\Delta\beta_{nq} \equiv \beta_n - \beta_q$. Note that the beat wavenumber is z dependent. A time dependence of the form $e^{+i\omega t}$ is assumed, where $i \equiv \sqrt{-1}$. In a future paper, we will show that reflected modes are negligible for all the cases considered here. The coupled-mode equations can be written in an

0018-9480/90/0600-0712$01.00

alternate form by defining

$$A_n^+(z) = \tilde{A}_n^+(z) e^{-i\int_0^z \beta_n(s)\,ds}.$$

Then

$$\frac{d\tilde{A}_n^+}{dz} = \sum_{\substack{q \\ q \neq n}} T_{nq}(z)\,\tilde{A}_q^+ e^{i\int_0^z (\beta_n - \beta_q)\,ds}. \tag{2}$$

III. Quasi-Periodic Mode Converters

In the initial stages of the design procedure for quasi-periodic TE_{0n}–TE_{0n-1} mode converters, we assume that the beat wavenumber is constant (independent of z) and consider only the TE_{0n}–TE_{0n-1} mode interaction. In later stages of the design procedure, we take into account the z dependence of the beat wavenumber and, for 60 GHz TE_{02}–TE_{01} mode transducers, include the five propagating TE_{0n} modes (TE_{01} through TE_{05}) in the numerical analysis. For the 150 GHz TE_{02}–TE_{01} mode transducer we include, in later stages of the design, seven propagating modes in the numerical analysis (TE_{01} through TE_{07}). Following Kovalev *et al.* [3], we examine mode transducers with a radius variation of the form

$$a(z) = a_1\{1 + (\epsilon_1/a_1)[1 \mp \cos(k_p z)]\} \tag{3}$$

where $a_1 = 0.01389$ m, ϵ_1/a_1 is the relative perturbation depth, and k_p is the guide perturbation wavenumber. For a two-period mode converter, $0 \leq k_p z \leq 4\pi$ and the upper sign in (3) is used. For a one-and-one-half-period mode converter, $0 \leq k_p z \leq 3\pi$ and the lower sign in (3) is used. More generally, the upper sign of (3) would be used for any even number of half perturbation periods and the lower sign for any odd number of half periods. This upper–lower sign convention is continued below in (4)–(8). The waveguide perturbation wavenumber, k_p, is approximately equal to the beat wavenumber. The coupled-mode equations for just the TE_{0n} and TE_{0n-1} modes far from cutoff (making $\beta_n/\beta_{n-1} \approx 1$) can be written in the form

$$\frac{d}{dz}\begin{bmatrix} \tilde{A}_{n-1}^+(z) \\ \tilde{A}_n^+(z) \end{bmatrix} = \frac{\pm 2\chi'_{0n}\chi'_{0n-1}}{\chi'^2_{0n} - \chi'^2_{0n-1}} \frac{(\epsilon_1/a_1)k_p \sin(k_p z)}{1 + (\epsilon_1/a_1)[1 \mp \cos(k_p z)]} \cdot \begin{bmatrix} 0 & e^{i\Delta\beta_{n,n-1}z} \\ -e^{-i\Delta\beta_{n,n-1}z} & 0 \end{bmatrix} \begin{bmatrix} \tilde{A}_{n-1}^+ \\ \tilde{A}_n^+ \end{bmatrix}. \tag{4}$$

An approximate solution to (4) can be found by assuming that

$$k_p = \Delta\beta_{n,n-1}$$

and

$$\frac{1}{1 + (\epsilon_1/a_1)[1 \mp \cos(k_p z)]} \simeq 1 - (\epsilon_1/a_1)[1 \mp \cos(k_p z)] + (\epsilon_1/a_1)^2[1 \mp \cos(k_p z)]^2 \tag{5}$$

TABLE I
Two-Mode Parameters

Initial Estimate		Final Result		TE_{01} Power at End of Converter
k_p	ϵ_1/a_1	k_p	ϵ_1/a_1	
		Two-Period Converter		
75.3 rad/m	0.188	79.8 rad/m	0.188	99.8%
		1-1/2 Period Converter		
75.3 rad/m	0.260	81.7 rad/m	0.261	99.8%

and neglecting rapidly varying phase terms in the expression

$$\sin(k_p z)\{1 - (\epsilon_1/a_1)[1 \mp \cos(k_p z)] + (\epsilon_1/a_1)^2 \cdot [1 \mp \cos(k_p z)]^2\} \begin{bmatrix} 0 & e^{i\Delta\beta_{n,n-1}z} \\ -e^{-i\Delta\beta_{n,n-1}z} & 0 \end{bmatrix}. \tag{6}$$

The approximate form for (4) is

$$\frac{d}{dz}\begin{bmatrix} \tilde{A}_{n-1}^+ \\ \tilde{A}_n^+ \end{bmatrix} = \frac{\pm i\chi'_{0n}\chi'_{0n-1}}{\chi'^2_{0n} - \chi'^2_{0n-1}} \Delta\beta_{n,n-1}\left(\frac{\epsilon_1}{a_1}\right) \cdot \left[1 - \left(\frac{\epsilon_1}{a_1}\right) + 5/4\left(\frac{\epsilon_1}{a_1}\right)^2\right] \begin{bmatrix} 0 & 1 \\ 1 & 0 \end{bmatrix} \begin{bmatrix} \tilde{A}_{n-1}^+ \\ \tilde{A}_n^+ \end{bmatrix}. \tag{7}$$

The solution of (7), assuming $\tilde{A}_n^+(0) = 1$ and $\tilde{A}_{n-1}^+(0) = 0$, is

$$\tilde{A}_{n-1}^+(z) = \pm i \sin\left\{\frac{\chi'_{0n}\chi'_{0n-1}}{\chi'^2_{0n} - \chi'^2_{0n-1}}(\epsilon_1/a_1) \cdot \left[1 - (\epsilon_1/a_1) + 5/4(\epsilon_1/a_1)^2\right]\Delta\beta_{n,n-1}z\right\} \tag{8}$$

and

$$\tilde{A}_n^+(z) = \cos\left\{\frac{\chi'_{0n}\chi'_{0n-1}}{\chi'^2_{0n} - \chi'^2_{0n-1}}(\epsilon_1/a_1) \cdot \left[1 - (\epsilon_1/a_1) + 5/4(\epsilon_1/a_1)^2\right]\Delta\beta_{n,n-1}z\right\}.$$

Complete mode conversion results when

$$\frac{\chi'_{0n}\chi'_{0n-1}}{\chi'^2_{0n} - \chi'^2_{0n-1}}\Delta\beta_{n,n-1}z_1(\epsilon_1/a_1) \cdot \left[1 - (\epsilon_1/a_1) + 5/4(\epsilon_1/a_1)^2\right] = \pi/2 \tag{9}$$

where z_1 is the length of the transducer ($\Delta\beta_{n,n-1}z_1 = 4\pi$ and 3π for the cases considered here).

Equation (4) was solved numerically for a two-period and a one-and-one-half-period TE_{02}–TE_{01} mode transducer. Initially we set k_p equal to the beat wavenumber and used (9) to estimate ϵ_1/a_1. With $\tilde{A}_1^+(0) = 0$ and $\tilde{A}_2^+(0) = 1$, both k_p and ϵ_1/a_1 were varied until an optimum solution (power in the TE_{01} mode close to 100% at the end of the transducer) was found. The results are given in Table I. The beat wavenumber was assumed to

be constant at 75.3 rad/m, which is the beat wavenumber for the TE_{02}–TE_{01} modes for a waveguide of radius 1.389 cm and frequency of operation of 60 GHz. Table I suggests that approximating k_p as $\Delta\beta_{n,n-1}$ and using (9) to obtain ϵ_1/a_1 yields reasonable estimates for an efficient mode coupling profile for the constant-beat-wavenumber, two-mode case.

For relatively long mode converters with correspondingly small perturbation amplitudes, the variation of the beat wavenumber has commonly been handled by averaging over the variation and using this average beat wavenumber (which is sometimes slightly varied to further increase efficiency) as the waveguide perturbation wavenumber [2]. At 60 GHz, this approach begins to break down for four-period converters. Some previous successful designs took this into account by using flat sections to improve efficiency [9]. In the present discussion, rather than using flat sections to improve efficiency, the two mode equations with variable beat wavenumber will be analyzed. A coupling profile of the form

$$a(z) = 0.01389\{1+(\epsilon_1/a_1)[1\mp\cos(H(z))]\} \quad \text{m} \quad (10)$$

will be used where, for the two-period device, $0 \leqslant H(z) \leqslant 4\pi$ and the minus sign in (10) is used; for the one-and-one-half-period device, $0 \leqslant H(z) \leqslant 3\pi$ and the plus sign in (10) is used. Using the radial variation given by (10) allows us to retain the amplitude estimate generated by the constant-beat-wavenumber case. The coupled-mode equations can be written in the form

$$\frac{d}{dz}\begin{bmatrix}\tilde{A}^+_{n-1}(z)\\ \tilde{A}^+_n(z)\end{bmatrix} = \frac{\pm i2\chi'_{0n}\chi'_{0n-1}}{\chi'^2_{0n}-\chi'^2_{0n-1}}(\epsilon_1/a_1) \cdot \frac{\sin(H(z))H'(z)}{\{1+(\epsilon_1/a_1)[1\mp(\epsilon_1/a_1)\cos(H(z))]\}} \cdot \begin{bmatrix}0 & e^{tj(\beta_{n-1}-\beta_n)ds}\\ -e^{-tj(\beta_{n-1}-\beta_n)ds} & 0\end{bmatrix} \cdot \begin{bmatrix}\tilde{A}^+_{n-1}(z)\\ \tilde{A}^+_n(z)\end{bmatrix}. \quad (11)$$

An equation for $H(z)$ can be derived by comparing (11) and (4). Noting in (4) that k_p is approximately equal to $\Delta\beta_{n,n-1}$ suggests that the variation of the beat wavenumber in (11) is accounted for if

$$\frac{dH}{dz} = \beta_{n-1}(z) - \beta_n(z) \quad (12)$$

where

$$\beta_{n-1}(z)-\beta_n(z) = k\left[\sqrt{1-\frac{\chi'^2_{0n-1}}{a_1^2k^2\{1+(\epsilon_1/a_1)[1\mp\cos(H(z))]\}^2}} - \sqrt{1-\frac{\chi'^2_{0n}}{a_1^2k^2\{1+(\epsilon_1/a_1)[1\mp\cos(H(z))]\}^2}}\right]. \quad (13)$$

Using the binomial theorem and taking advantage of the fact that the waveguide is highly overmoded and hence

$$\frac{\chi'^2_{0n}}{a_1^2k^2\{1+(\epsilon_1/a_1)[1\mp\cos(H(z))]\}^2} \ll 1$$

we can approximate (13) as

$$\frac{dH}{dz} \simeq \frac{\chi'^2_{0n}-\chi'^2_{0n-1}}{2ka_1^2\{1+(\epsilon_1/a_1)[1\mp\cos(H(z))]\}^2} \cdot \left\{1+\frac{\chi'^2_{0n}+\chi'^2_{0n-1}}{4a_1^2k^2[1+(\epsilon_1/a_1)]^2}\right\}. \quad (14)$$

Using a perturbational approach, we can solve (14) approximately. Assuming $H(z) = H_0(z) + H_1(z)$, where $H_0(z) > H_1(z)$, $\cos(H(z)) \simeq \cos(H_0) - H_1\sin(H_0)$, and $\cos(2H(z)) \simeq \cos(2H_0) - 2H_1\sin(2H_0)$ leads to

$$\left[1+2(\epsilon_1/a_1)+3/2(\epsilon_1/a_1)^2\right]\left(\frac{dH_0}{dz}+\frac{dH_1}{dz}\right) + \left\{\mp2\left[(\epsilon_1/a_1)+(\epsilon_1/a_1)^2\right] \cdot[\cos(H_0)-H_1\sin(H_0)]\right\}\left(\frac{dH_0}{dz}+\frac{dH_1}{dz}\right) + 1/2(\epsilon_1/a_1)^2[\cos(2H_0)-2H_1\sin(2H_0)] \cdot\left(\frac{dH_0}{dz}+\frac{dH_1}{dz}\right) \simeq \frac{\chi^2_{0n}-\chi'^2_{0n-1}}{2ka_1^2} \cdot\left\{1+\frac{\chi'^2_{0n}+\chi'^2_{0n-1}}{4a_1^2k^2[1+(\epsilon_1/a_1)]^2}\right\}.$$

If we assume

$$\left[1+2(\epsilon_1/a_1)+3/2(\epsilon_1/a_1)^2\right]\frac{dH_0}{dz} = \frac{\chi'^2_{0n}-\chi'^2_{0n-1}}{2ka_1^2}\left\{1+\frac{\chi'^2_{0n}+\chi'^2_{0n-1}}{4a_1^2k^2[1+(\epsilon_1/a_1)]^2}\right\}$$

$$2\left((\epsilon_1/a_1)+(\epsilon_1/a_1)^2\right)\left(-H_1\sin(H_0)\frac{dH_1}{dz}\right) \simeq 0$$

and

$$(\epsilon_1/a_1)^2[-2H_1\sin(2H_0)]\frac{dH_1}{dz} \simeq 0$$

the solution for $H(z)$ is

$$H_0(z) = \frac{z}{1+2(\epsilon_1/a_1)+3/2(\epsilon_1/a_1)^2}\frac{\chi'^2_{0n}-\chi'^2_{0n-1}}{2ka_1^2} \cdot\left\{1+\frac{\chi'^2_{0n}+\chi'^2_{0n-1}}{4a_1^2k^2[1+(\epsilon_1/a_1)]^2}\right\} \quad (15)$$

and

$$H_1(z) = \frac{\pm 2\left[(\epsilon_1/a_1)+(\epsilon_1/a_1)^2\right]\sin(H_0) - 1/4(\epsilon_1/a_1)^2\sin(2H_0)}{1+2\epsilon_1/a_1+3/2(\epsilon_1/a_1)^2 \mp 2\left[\epsilon_1/a_1+(\epsilon_1/a_1)^2\right]\cos(H_0)+1/2(\epsilon_1/a_1)^2\cos(2H_0)}. \quad (16)$$

The upper sign in (16) is for a two-period device and the lower sign in (16) is for a one-and-one-half-period device. The term $[\epsilon_1/a_1 + (\epsilon_1/a_1)^2]\cos(H_0) + 1/2(\epsilon_1/a_1)^2\cos(2H_0)$ had a negligible effect on conversion efficiency and was neglected. Using (9), (15), and (16) as initial estimates, we designed a two-period 60 GHz mode converter. The TE_{01} through TE_{05} modes were used in the numerical analysis. After numerically optimizing the parameters, the transducer had a numerically calculated efficiency of 96%. The efficiency was further increased by empirically altering the perturbation profile slightly. A two-period TE_{02}–TE_{01} mode transducer with radial variation

$$\begin{aligned} a(z) = 0.01389\{1+0.188[1-0.06 &\cdot\cos[44.9z-0.3\sin(51.0z)]] \\ &\cdot[1-\cos(51.0z+0.45\sin(51.0z) \\ &+0.1\sin(102.0z))]\} \quad \text{m} \end{aligned} \quad (17)$$

was found to have a computed conversion efficiency of 99.6%. (Conversion efficiency is defined as the ratio of the power out of a mode converter in the desired mode to the total input power, here taken to be in a single mode. Losses are included.) Note that the efficiency is lower than that listed in Table I because five propagating modes, TE_{01} through TE_{05}, were included in the numerical analysis here. Fig. 1 is a plot of the mode amplitudes of the first five TE_{0n} modes in the two-period converter versus normalized position (z/average perturbation period). Similarly, a one-and-one-half-period 60 GHz transducer with a radius variation

$$\begin{aligned} a(z) = 0.01389\{1+0.271[1-0.14\cos(17.1z)] \\ \cdot[1+\cos(42.7z-0.35\sin(42.7z))]\} \quad \text{m} \end{aligned} \quad (18)$$

has a numerically calculated efficiency of 99.6%. Fig. 2 is a plot of the mode amplitudes of the first five TE_{0n} modes in the one-and-one-half-period converter versus position. Fig. 3 shows the conversion efficiency as a function of frequency of the two-period and one-and-one-half-period devices compared with that of a pioneering design by Moeller [1].

Recently, Thumm *et al.* [4] developed a two-period 150 GHz TE_{02}–TE_{01} mode converter with a constant perturbation wavenumber. They used a radial profile of the form

$$a(z) = 0.01389[1+0.1606\cos(19.5z)]/1.1606 \quad \text{m}. \quad (19)$$

This device is highly efficient (99.5%). However, the radius is substantially less than 0.01389 m in places and, due to the large TE_{02}–TE_{01} beat wavenumber variation, this constant-perturbation-wavenumber technique does not work well at 60 GHz. Using the techniques developed in this paper, we have designed a one-and-one-half-period TE_{02}–TE_{01} 150 GHz mode transducer. The radial variation is

$$\begin{aligned} a(z) = 0.01389\{1+0.283[1-0.09\cos(6.6z)] \\ \cdot[1+\cos(16.5z-0.22\sin(16.5z))]\} \quad \text{m}. \end{aligned} \quad (19')$$

The device is 0.571 m long and has an efficiency of 99.5%, including losses.

IV. Aperiodic Mode Converters (Combined Mode Converters and Tapers)

In a periodic or quasi-periodic TE_{0n}–TE_{0n-1} mode converter, viewed somewhat simplistically, the sign of the slope of the radius perturbation must be changed near the points where power would begin to flow back out of the TE_{0n-1} mode to which it had been transferring. This change in sign of the radius slope must occur at zero-slope points to avoid slope discontinuities. The change in the sign of the radius slope changes the sign of the coupling coefficients and keeps the power transferring to the TE_{0n-1} mode. Approximately the same effect may be obtained by inserting a straight section of uniform waveguide at these zero-slope inversion points and then continuing the radius perturbation without a change in the sign of the slope, which we refer to as *unfolding*. This produces a combined mode converter and taper. The length of the section of uniform waveguide should be approximately one half the beat wavelength between the input mode and the desired output mode. Waveguide radius tapers are commonly used in mode converter systems because shorter, higher-conversion-efficiency mode transducers (particularly TE_{01}–TE_{11} converters) are possible in waveguides of smaller radius.

The basis for the aperiodic TE_{0n}–TE_{0n-1} mode converters can be seen by examining Fig. 4. Fig. 4(a) shows a taper and a two-period mode transducer. Fig. 4(b) shows the diameter variation of a conventional one-and-one-half-period device "unfolded" with two constant-radius sections half a beat wavelength long inserted between each curved section. This aperiodic device is substantially shorter than the combined length of the taper and two-period mode converter.

Consider the integral form of the coupled-mode equations where we assume that only the TE_{0n} and TE_{0n-1} modes are interacting in a highly overmoded waveguide:

$$\frac{d\tilde{A}^+_{n-1}}{dz} = \frac{2\chi'_{0n}\chi'_{0n-1}}{\chi'^2_{0n}-\chi'^2_{0n-1}}\frac{1}{a}\frac{da}{dz}\tilde{A}^+_n(z)e^{\iota\int_0^z[\beta_{n-1}(s)-\beta_n(s)]ds} \quad (20)$$

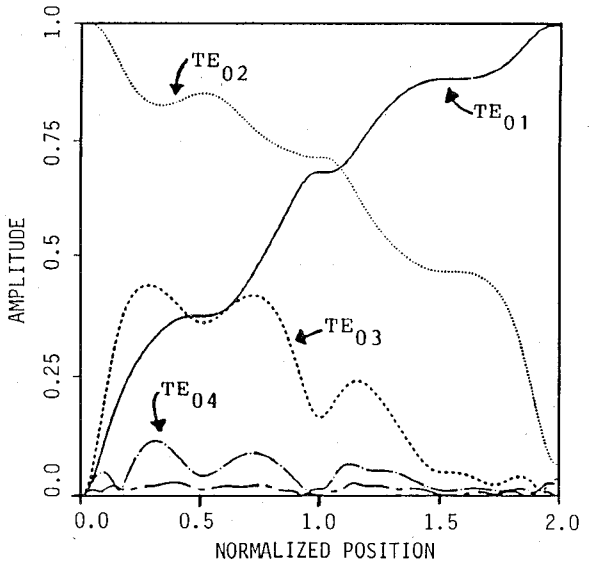

Fig. 1. Modal amplitude as a function of normalized position for a 99.6% efficient two-period 60 GHz TE_{02}–TE_{01} mode converter.

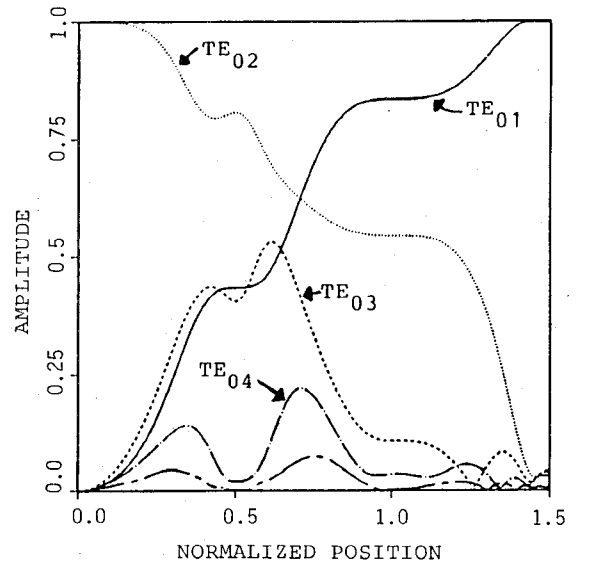

Fig. 2. Modal amplitude as a function of normalized position for a 99.6% efficient one-and-one-half-period 60 GHz TE_{02}–TE_{01} mode converter.

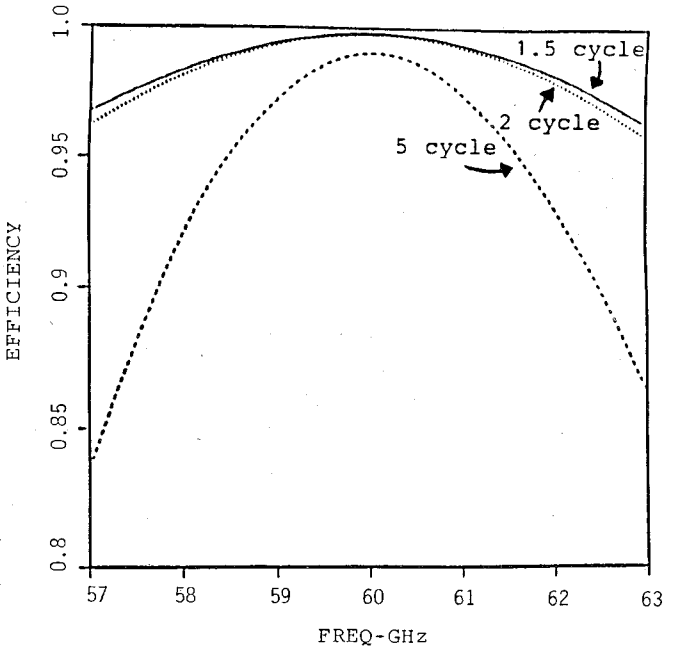

Fig. 3. Conversion efficiency of the one-and-one-half-period and two-period designs for 60 GHz TE_{02}–TE_{01} mode converters as a function of frequency compared with the pioneering five-period design by Moeller [1].

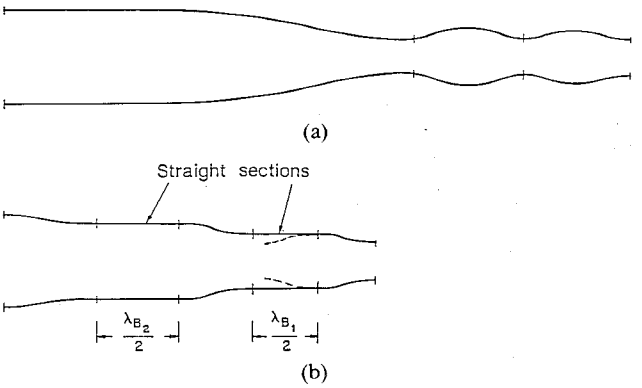

Fig. 4. (a) A down-taper and a TE_{03}–TE_{02} mode converter compared with (b) an unfolded aperiodic mode converter combining both of these functions and having a shorter length than previous down-tapers alone.

and

$$\frac{d\tilde{A}_n^+}{dz} = \frac{-2\chi'_{0n}\chi'_{0n-1}}{\chi'^2_{0n} - \chi'^2_{0n-1}} \frac{1}{a}\frac{da}{dz} \tilde{A}_{n-1}^+(z) e^{-i\int_0^z [\beta_{n-1}(s) - \beta_n(s)]ds}. \tag{21}$$

For a conventional one-and-one-half-period mode converter, the radial perturbations have the approximate form

$$a(z) = a_1\{1 + (\epsilon_1/a_1)[1 + \cos(H(z))]\} \tag{22}$$

where $0 \leqslant H(z) \leqslant 3\pi$, $dH/dz = \beta_{n-1}(z) - \beta_n(z)$, and ϵ_1/a_1 (the relative perturbation amplitude) is constant. For an "unfolded" one-and-one-half-period device $\frac{1}{a}\frac{da}{dz} \leqslant 0$ over the entire length of the device. For the conventional "folded" one-and-one-half-period device for $\pi < H(z) < 2\pi$ (second half period), $-\frac{1}{a}\frac{da}{dz} \geqslant 0$. If a constant-radius section half a beat wavelength long is inserted between the first and second curved sections of the "unfolded" one-and-one-half-period device, the coupled-mode equations of the aperiodic device are nearly identical to the coupled-mode equations of the conventional one-and-one-half-period device; hence efficient mode conversion takes place. Similarly, a constant-radius section half a beat wavelength long must be inserted between the second and third perturbed sections in order for efficient mode conversion to take place.

We used the unfolding technique to design two mode transducers: a 60 GHz TE_{02}–TE_{01} mode converter–taper and a 140 GHz TE_{03}–TE_{01} mode converter–taper. In each case, the taper had to be from a 6.35-cm-diameter

TABLE II
RADIAL VARIATION OF THE 140 GHz TE_{03}–TE_{02} CONVERTER–TAPER

First Curved Section (for z_1 in m):
$a(z_1) = 0.024461\{1 + 0.149[1 + \cos[9.6z_1 - 0.28\sin(9.6z_1)/(1 + 0.38\cos(9.6z_1))]]\}$ m
$0 \leqslant 9.6z_1 \leqslant \pi$; length of first constant-radius section = 0.2016 m.

Second Curved Section (z_2 in m, $z_2 = 0$ at end of first constant-radius section):
$a(z_2) = 0.01914\{1 + 0.139[1 + \cos[20.4z_2 - 0.36\sin(20.4z_2)/(1 + 0.46\cos(20.4z_2))]]\}$ m
$0 \leqslant 20.4z_2 \leqslant \pi$; length of second constant-radius section = 0.1228 m.

Third Curved Section (z_3 in m, $z_3 = 0$ at end of second constant-radius section):
$a(z_3) = 0.014522\{1 + 0.159[1 + \cos[34.0z_3 - 0.36\sin(34.0z_3)/(1 + 0.25\cos(34.0z_3))]]\}$ m
$0 \leqslant 34.0z_3 < \pi$.

waveguide to a 2.778-cm-diameter waveguide. The 140 GHz taper–converter has the TE_{02} mode as an intermediate step. As Thumm *et al.* [4] point out, the TE_{04}–TE_{03} beat wavenumber is quite close to the TE_{03}–TE_{01} beat wavenumber; hence direct TE_{03}–TE_{01} mode conversion appears intractable.

Each unfolded section of the ideal mode converter–taper has the radial variation $a(z) = a_1\{1 + (\epsilon_1/a_1)[1 + \cos(H(z))]\}$, where $0 \leqslant H(z) \leqslant \pi$. Equation (9) can be used to generate an estimate for ϵ_1/a_1. For the 140 GHz TE_{03}–TE_{01} device, the basis for the tapered portion of the device is a one-and-one-half-period TE_{03}–TE_{02} mode converter. The unfolded one-and-one-half-period device tapers from a 6.35-cm-diameter waveguide to nearly the desired 2.779-cm-diameter waveguide. For the 60 GHz TE_{02}–TE_{01} mode transducer, an unfolded one-and-one-half-period device would taper from a much greater diameter than 6.35 cm to 2.779 cm. However, we found that a partially unfolded two-period device with one cycle unfolded to taper from 6.35 cm to 2.779 cm and the other cycle of conventional form was a good basis for the design of a 60 GHz TE_{02}–TE_{01} mode converter–taper.

The design of the 140 GHz mode converter–taper began with the design of the TE_{03}–TE_{02} taper. The objective in the design of the TE_{03}–TE_{02} taper was to make the TE_{02} content large at the end of the taper while minimizing the content in the TE_{04} or higher modes. Equations (15) and (16) served as an initial estimate for the parameters of the tapered portion of the device. In contrast to the quasi-periodic devices, the term $2[\epsilon_1/a_1 + (\epsilon_1/a_1)^2]\cos(H_0(z))$ was retained. The perturbation amplitude of each section of the taper was varied, the only restriction being that the taper not exceed the initial and final diameters of 6.35 cm and 2.779 cm. Eight modes (TE_{01} through TE_{08}) were used in the numerical calculations. Table II lists the radial variation of the TE_{03}–TE_{02} converter–taper portion of the 140 GHz device and the length of the two flat sections. Table III lists the modal output of the TE_{03}–TE_{02} converter–taper. Note that the diameter at the end of the TE_{03}–TE_{02} converter–taper is slightly larger than 2.779 cm.

The next step in the process was to design a half-period converter which would taper the waveguide diameter from 0.02904 m to 0.02779 m and increase the power in the first three modes. A mode coupling profile of the form

$$a(z) = 0.01389\{1 + 0.02275[1 + \cos(H(z))]\} \text{ m} \quad (23)$$

TABLE III
MODAL POWER AT END OF TE_{03}–TE_{02} CONVERTER–TAPER

Mode	% Power
TE_{01}	4.23
TE_{02}	94.27
TE_{03}	0.56
TE_{04}	0.58
TE_{05}	0.001
TE_{06}	0.31
TE_{07}	0.004
TE_{08}	0.002

where $0 \leqslant H(z) \leqslant \pi$, was chosen. There are a number of different choices for $H(z)$ depending on whether mode conversion is attempted between the TE_{02} and TE_{01} modes, TE_{03} and TE_{02} modes, TE_{04} and TE_{03} modes, or possibly some other combination of modes. Through a trial-and-error process, we determined that a good choice for $H(z)$ in (23) was based on mode conversion between the TE_{04} and TE_{03} modes. Since ϵ_1/a_1 was quite small, $H(z)$ was set equal to the approximate TE_{03}–TE_{04} beat wavenumber times z, $62.3z$. With this choice of $H(z)$, the total power of the first three TE_{0n} modes at the end of the small taper increased slightly. Alternative design strategies resulted in the power in the TE_{04} mode at the end of the TE_{03}–TE_{02} mode converter coupling to higher order modes. In the following TE_{02}–TE_{01} mode converter, it was difficult to empirically alter the device slightly to couple this power to the TE_{01} mode.

The modal output of the small TE_{04}–TE_{03} converter was then the input for a two-period converter. Since the largest fraction of the input power was in the TE_{02} mode, a TE_{02}–TE_{01} mode converter design served as an initial estimate for the converter parameters. After optimizing the parameters, the radial variation is

$$\begin{aligned} a(z) = 0.01389\{&1 + 0.169 \\ &\cdot[1 - 0.14\sin(7.5z - 0.3\sin(21.5z))] \\ &\cdot[1 - 0.04\sin(17.2z - 0.3\sin(21.5z))] \\ &\cdot[1 + 0.02\sin(25.8z)] \\ &\cdot[1 - \cos(21.5z + 0.43\sin(21.5z) + \\ &+ 0.15\sin(43.0z))]\} \text{ m} \end{aligned}$$

where $0 \leqslant 21.5z \leqslant 4\pi$.

The efficiency of the 140 GHz TE_{03}–TE_{01} mode converter–taper is 99.4%. Fig. 5 shows the amplitude varia-

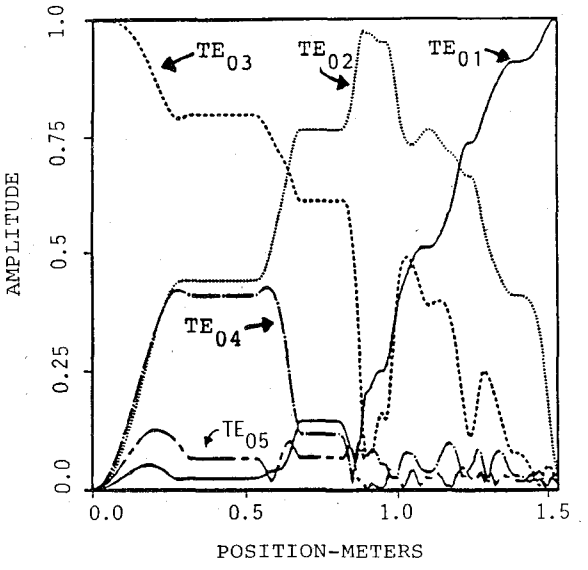

Fig. 5. Modal amplitude as a function of position for a 99.4% efficient 140 GHz mode converter–taper. This device tapers from a 6.35 cm waveguide diameter to a 2.779 cm waveguide diameter.

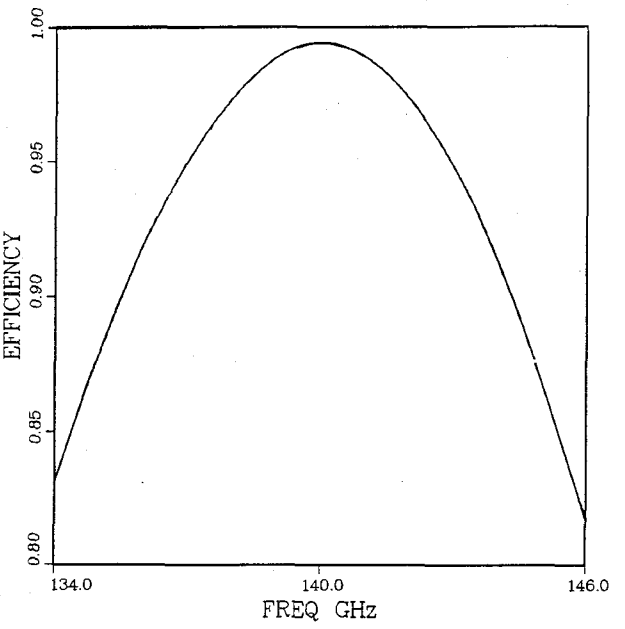

Fig. 6. Conversion efficiency of the 140 GHz mode converter–taper as a function of frequency.

tion of the TE_{0n} modes versus the length of the TE_{03}–TE_{01} converter–taper and Fig. 6 is a plot of its conversion efficiency as a function of frequency.

For the 60 GHz TE_{02}–TE_{01} converter–taper, we arbitrarily unfolded one period to taper from a 6.35-cm-diameter waveguide to a 2.779-cm-diameter waveguide. The mode conversion was completed with a folded period. Initially we assumed that each half-period of the unfolded period had equal perturbation amplitude. The initial estimate of the perturbation amplitude of the folded period was obtained from two mode considerations.

The exact solution for the two-mode constant-beat-wavenumber case (eq. (4)) is

$$|\tilde{A}^+_{n-1}(z)| = \left|\sin\left\{\int_0^z f(s)\cos\left[\delta_n(s) - \delta_{n-1}(s) + \Delta\beta_{n,n-1}s\right]ds\right\}\right|$$

where

$$\tilde{A}^+_{n-1}(z) = |\tilde{A}^+_{n-1}(z)|e^{i\delta_{n-1}(z)},\quad \tilde{A}^+_n(z) = |\tilde{A}^+_n(z)|e^{i\delta_n(z)}$$

$$f(z) = \frac{\pm 2(\chi'_{0n}\chi'_{0n-1})(\epsilon_1/a_1)k_p\sin(k_pz)}{\left[\chi'^2_{0n} - \chi'^2_{0n-1}\right]\left\{1+(\epsilon_1/a_1)\left[1\mp\cos(k_pz)\right]\right\}}$$

$$\delta_{n-1}(z) = \delta_{n-1}(0) + \int_0^z f(s)\frac{\sqrt{1-|A^+_{n-1}(s)|^2}}{|A^+_{n-1}(s)|}\cdot\sin\left[\delta_n(s) - \delta_{n-1}(s) + \Delta\beta_{n,n-1}s\right]ds$$

and

$$\delta_n(z) = \delta_n(0) + \int_0^z f(s)\frac{|A^+_{n-1}(s)|}{\sqrt{1-|A_{n-1}(s)|^2}}\cdot\sin\left[\delta_n(s) - \delta_{n-1}(s) + \Delta\beta_{n,n-1}s\right]ds.$$

In the expression for $f(z)$, the upper sign is for a two-period device and the lower sign is for a one-and-one-half-period device. If we assume that the modes are 90° out of phase (consistent with (8)) and that $\Delta\beta_{n,n-1} = k_p$ and we use the binomial theorem, the expression for the perturbation amplitudes is

$$\frac{\chi'_{0n}\chi'_{0n-1}}{\chi'^2_{0n} - \chi'^2_{0n-1}}\sum_i \Delta\beta_{n,n-1}z_{1i}(\epsilon_{1i}/a_1)\cdot\left[1-\epsilon_{1i}/a_1 + 5/4(\epsilon_{1i}/a_1)^2\right] = \frac{\pi}{2}$$

where z_{1i} is the length of each section of the transducer and ϵ_{1i}/a_1 is the perturbation amplitude of each section of the transducer. The summation is over all sections of the transducer. For the 60 GHz taper–transducer, $\Delta\beta_{21}z_{11} = \Delta\beta_{21}z_{12} = \pi$, $\epsilon_{11}/a_1 = \epsilon_{12}/a_1 = 0.2559$, and $\Delta\beta_{21}z_{13} = 2\pi$. Thus ϵ_{13}/a_1 could be determined. Once the perturbation amplitudes were determined, (15) and (16) were used to determine initial estimates for $H_0(z)$ and $H_1(z)$.

After the parameters were numerically optimized, the theoretical efficiency of the device was 99.4%. Ohmic losses were included in the calculation. The radial variation of the 60 GHz TE_{02}–TE_{01} mode transducer–taper is given in Table IV.

The second perturbed section of the taper and the folded transducer have unexpected values for $H_1(z)$. This is due to the change in curvature between the first and second periods of the device. Fig. 7 is a plot of modal amplitude versus distance down the converter. Fig. 8 is a plot of conversion efficiency as a function of frequency for the 60 GHz mode converter–taper.

V. Experiment Results

The 60 GHz TE_{02}–TE_{01} two-period mode converter discussed in Section III and the 60 GHz TE_{02}–TE_{01} mode converter–taper discussed in Section IV were fabri-

TABLE IV
RADIAL VARIATION OF THE 60 GHz TE_{02}-TE_{01} MODE CONVERTER-TAPER

First Perturbed Section (z_1 in m):

$$a(z_1) = 0.021198\{1 + 0.244[1 + 0.02\cos(10.4z_1)] \cdot [1 + \cos(17.3z_1 - 0.38\sin(17.3z_1)/(1 + 0.35\cos(17.3z_1)) - 0.02\sin(34.6z_1))]\} \text{ m}$$

$0 \leq 17.3z_1 \leq \pi$; length of flat section = 0.1003 m.

Second Perturbed Section (z_2 in m):

$$a(z_2) = 0.01389\{1 + 0.2522[1 + 0.04\cos(9.38z_2)] \cdot [1 + \cos(46.9z_2 + 0.24\sin(46.9z_2)/(1 + 0.36\cos(46.9z_2)) + 0.04\sin(93.8z_2))]\} \text{ m}$$

$0 \leq 46.9z_2 \leq \pi$.

Third Perturbed Section (z_3 in m):

$$a(z_3) = 0.01389\{1 + 0.143[1 - 0.2\cos(41.4z_3)] \cdot [1 - \cos(63.7z_3 - 0.09\sin(63.7z_3)/(1 + 0.12\cos(63.7z_3)) + 0.17\sin(127.4z_3))]\} \text{ m}$$

$0 \leq 63.7z_3 \leq 2\pi$.

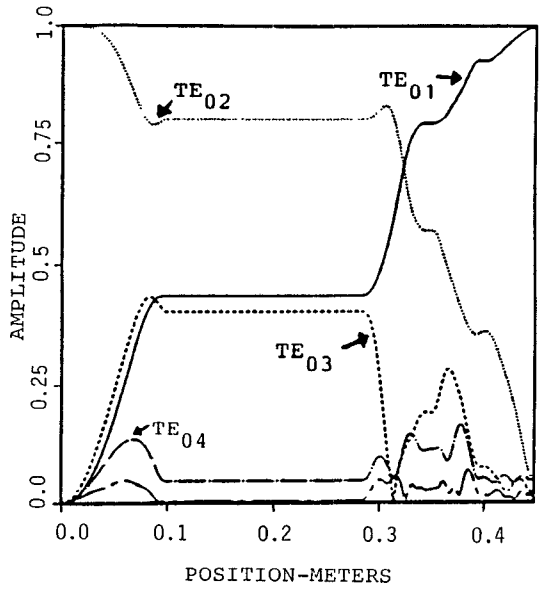

Fig. 7. Modal amplitude as a function of position for a 99.4% efficient 60 GHz mode converter-taper. This device tapers from a 6.35 cm waveguide diameter to a 2.779 cm waveguide diameter.

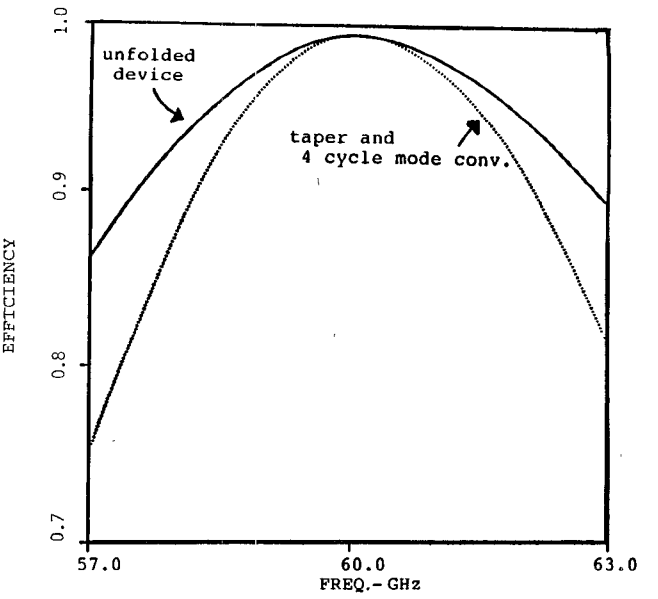

Fig. 8. Plot of conversion efficiency as a function of frequency for the "unfolded" 60 GHz converter-taper and a taper followed by a four-period mode converter.

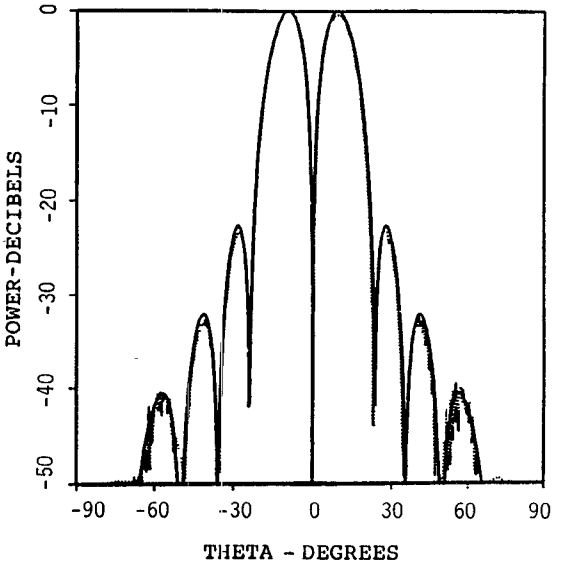

Fig. 9. Plot of theoretical (solid line) and experimental (dotted line) results for the TE_{01} mode radiating from the open end of a 2.779-cm-diameter waveguide. The aperture-to-receiver distance was 160 cm.

cated and their approximate conversion efficiencies were measured at low power. This was done by feeding a TE_{01} mode *into* the normal TE_{01} mode *output* end and measuring the E_ϕ radiation patterns of both the TE_{01} input and the TE_{02} output modes. The mode purity of each of these modes can be determined to within about 1% from these open-end radiation patterns [2], [11]. From the Lorentz reciprocity theorem [10], the percentage of TE_{02} mode out for a TE_{01} mode in at the TE_{01} mode end is the same as the percentage of TE_{01} mode out for a TE_{02} mode in at the TE_{02} end. Since we are considering TE_{0n} modes in highly overmoded waveguides, losses are of the order of only 0.1%. Thus, for a high-purity TE_{01} mode input, the conversion efficiency is approximately equal to the fraction of the TE_{02} mode out.

The circular waveguide TE_{01} mode input into the converters was obtained by using a mode transducer which converts a rectangular waveguide TE_{10} mode to a circular waveguide TE_{01} mode followed by a circular waveguide mode filter, both of which are commercially available. The circular waveguide diameter of these devices was only 0.968 cm, so a special up-taper was designed[1] to taper to the necessary 2.779 cm diameter. The output from the circular waveguide up-taper was tested by measuring the radiation pattern from its open 2.779 cm end. Fig. 9 is a comparison of the theoretical and experimental results for the E_ϕ component of the far field of the TE_{01} mode radiation pattern. The TE_{01} mode at the 2.779 cm end was better than 99% pure and served as a source for the testing of the two mode converters.

[1]The design of the TE_{01} up-taper was begun by J. Shafii.

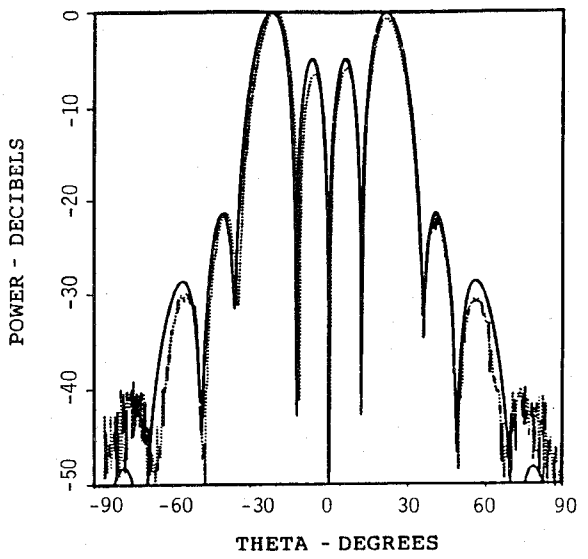

Fig. 10. Plot of theoretical (solid line) and experimental (dotted line) radiation patterns from the two-period TE_{02}–TE_{01} mode converter. The aperture-to-receiver distance was 160 cm.

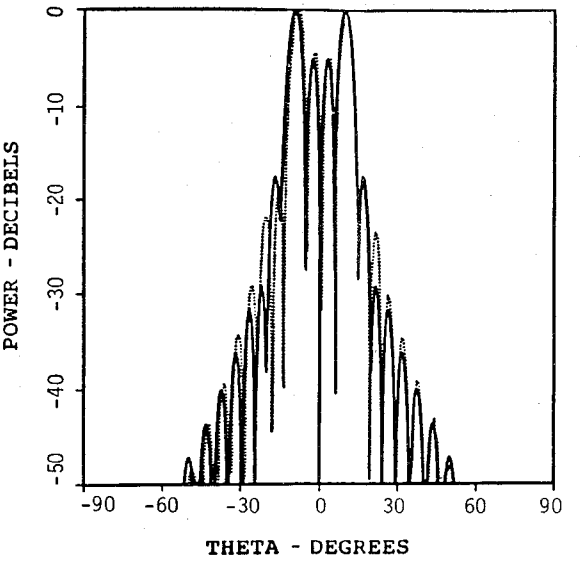

Fig. 12. Plot of theoretical (solid line) and experimental (dotted line) radiation patterns from the 6.35 cm end of the 60 GHz mode converter–taper. The aperture-to-receiver distance was 160 cm.

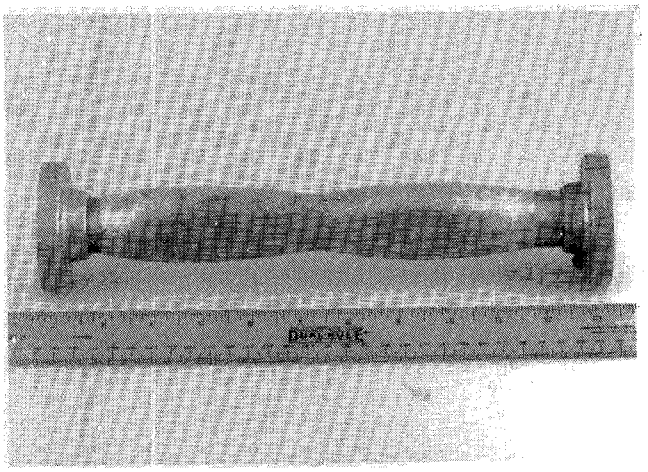

Fig. 11. Photograph of the two-period 60 GHz TE_{02}–TE_{01} mode converter.

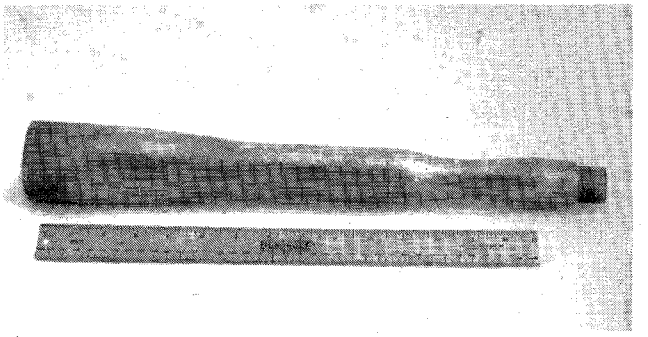

Fig. 13. Photograph of the 6.35 cm–2.779 cm 60 GHz TE_{02}–TE_{01} mode converter–taper.

Fig. 10 is a comparison of the theoretical and experimental results for the E_ϕ component of the far-field radiation pattern of the TE_{02} mode output from the two-period TE_{01}–TE_{02} mode converter. The theoretical radiation pattern in Fig. 10 is a superposition of the radiation patterns of all the modes present with significant amplitude as determined by numerically integrating the coupled-mode equations. Agreement between theory and experiment is reasonably good. The percentage of TE_{02} mode is greater than 99%. Fig. 11 is a photograph of the two-period mode converter.

In order to test the 60 GHz 6.35–2.779 cm TE_{02}–TE_{01} mode converter–taper, the TE_{01} mode was applied to the 2.779 cm end. Fig. 12 is a comparison of the experimental and theoretical E_ϕ radiation patterns for the 6.35-cm-diameter waveguide output when a TE_{01} mode is incident at the 2.779 cm end. Agreement between theory and experiment is reasonably good. The percentage of TE_{02} mode is greater than 98%. Fig. 13 is a photograph of the 6.35–2.779 cm TE_{02}–TE_{01} mode converter–taper.

VI. Conclusion

Designs of compact quasi-periodic and aperiodic circular waveguide mode converters for use in an electron cyclotron heating (ECH) system have been developed by analytically and numerically solving the coupled-mode differential equations. Experimental results are consistent with theoretical results. The theoretical efficiency of a two-period TE_{02}–TE_{01} mode converter with a length of 24.9 cm is 99.6%. The aperiodic mode converter–tapers combine a 6.35 cm–2.779 cm diameter taper and a mode converter. The 60 GHz TE_{02}–TE_{01} mode converter has a theoretical efficiency of 99.4% and is 44.7 cm long. The 140 GHz TE_{03}–TE_{01} aperiodic mode converter–taper has a theoretical efficiency of 99.4% and is 148 cm long. The techniques presented here are applicable to a variety of high-power overmoded mode converters.

REFERENCES

[1] C. Moeller, "Mode converters used in the doublet III ECH microwave system," *Int. J. Electron.*, vol. 53, p. 587, 1982.

[2] M. Thumm, "High-power millimeter-wave mode converters in overmoded circular waveguides using periodic wall perturbations," *Int. J. Electron.*, vol. 57, p. 1225, 1984.

[3] N. F. Kovalev, I. M. Orlova, and M. I. Peletin, "Wave transformation in a multimode waveguide with corrugated walls," *Radio Physics, Quant. Electron.*, vol. 11, pp. 449–450, 1969.

[4] M. Thumm, H. Kumric, and H. Stickel, "TE_{03} to TE_{01} mode converters for use with a 150 GHz gyrotron," *Int. J. Infrared and Millimeter Waves*, vol. 8, p. 227, 1987.

[5] M. J. Buckley, G. H. Luo, and R. J. Vernon, "New compact quasi-periodic and aperiodic mode converters for 60 and 140 GHz," presented at 12th Int. Conf. Infrared and Millimeter Waves, Lake Buena Vista, FL, Dec. 1987.

[6] M. J. Buckley, G. H. Luo, and R. J. Vernon, "New compact broadband high-efficiency mode converters for high power microwave tubes with TE_{0n} or TM_{0n} mode outputs," presented at IEEE MTT-S Int. Microwave Symposium, New York, NY, May 1988.

[7] H-G. Unger, "Circular waveguide taper of improved design," *Bell Syst. Tech. J.*, vol. 37, p. 912, 1958.

[8] S. A. Schelkunoff, "Conversion of Maxwell's equations into generalized telegraphists equations," *Bell Syst. Tech. J.*, vol. 34, pp. 995–1043, 1955.

[9] U. D. Rhee, Ph.D. thesis, University of Wisconsin-Madison, 1985, p. 67.

[10] R. Bellman and G. M. Wing, *An Introduction to Invariant Imbedding*. New York: Wiley, 1975.

[11] R. J. Vernon, W. R. Pickles, M. J. Buckley, F. Firouzbakht, and J. A. Lorbeck, "Mode content determination in overmoded circular waveguides by open-end radiation pattern measurement," presented at IEEE Int. *Symp.* Antennas and Propagation, Blacksburg, VA, June 1987.

[12] R. E. Collin, *Foundations for Microwave Engineering*. New York: McGraw-Hill, 1966.

Michael J. Buckley (S'88–M'88) received the B.S. degree in physics from the College of William and Mary in 1982 and the M.S. and Ph.D. degrees in electrical engineering from the University of Wisconsin in 1984 and 1988 respectively. At the University of Wisconsin his research interests included mode coupling in overmoded waveguides and radiation from overmoded waveguides.

In August 1988, he joined the Antenna Department of Texas Instruments in McKinney, TX.

✠

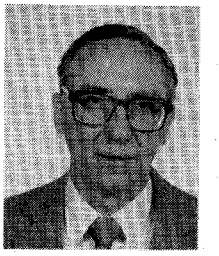

Ronald J. Vernon (S'64–M'65) was born in Chicago, IL, on June 3, 1936. He received the B.S., M.S., and Ph.D. degrees in electrical engineering from Northwestern University, Evanston, IL, in 1959, 1961, and 1965 respectively.

He worked under a cooperative student program in the Remote Control Engineering Division of Argonne National Laboratory from 1955 to 1958. Later he worked during the summer as an electrical engineer for the Communications and Industrial Electronics Division of Motorola Inc. Since 1965, he has been on the faculty of the University of Wisconsin, Madison, where he is presently a Professor of Electrical and Computer Engineering. In 1976–77 he took a leave of absence to work at the Lawrence Livermore National Laboratory. His current research interests are in the development of transmission and mode conversion systems for high-power microwave tubes such as gyrotrons.

Dr. Vernon is a member of Sigma Xi, Tau Beta Pi, Eta Kappa Nu, and Pi Mu Epsilon.